RASĀYAN *J. Chem.*
Vol. 15 | No. 2 |1212-1219| April - June | 2022
ISSN: 0974-1496 | e-ISSN: 0976-0083 | CODEN: RJCABP
http://www.rasayanjournal.com
http://www.rasayanjournal.co.in

ACTIVATION OF ZINC-PHOSPHATE WITH SILVER FOR ENHANCED ANTIMICROBIAL ACTIVITY

A.L. Arunachalam[1], P.S. Raghavan[1], S. Induja[1] and V. Parthasarathy[2,✉]
[1]Department of Chemistry, Hindustan Institute of Technology and Science,
Padur, Chennai-603103, TN, India
[2]Department of Physics, Hindustan Institute of Technology and Science,
Padur, Chennai-603103, TN, India
✉Corresponding Author: parthu0406@gmail.com

ABSTRACT
Zinc phosphate was doped with silver to enhance its antibacterial potential. The samples were prepared by co-precipitation technique in the presence of suitable surfactant and analyzed using XRD, SEM, and FTIR physico-chemical techniques. The prepared sample was analyzed to assess its antibacterial properties against *S. aureus* and *E. coli*. The antifungal activity was evaluated against *S. cerevisiae* and *A. brasiliensis* and compared with that of zinc phosphate. Around a 5-fold increase in antimicrobial activity was observed with a silver activated zinc phosphate than that over the blank.
Keywords: Zinc Phosphate, Antifungal Activity, Antimicrobial Activity, SEM, Silver.
RASĀYAN*J. Chem.*, Vol. 15, No.2, 2022

INTRODUCTION

Non-development of resistance by microorganisms against inorganic agents attracted various research groups around the world to find materials that exhibit activity equivalent to that of organic agents. Metals and metal oxides of silver, copper, and zinc in the form of nanoparticles exhibit very high activity, but the environmental toxicity of these smaller particles triggers scientists to find new lesser toxic materials. The zinc compounds are generally safe for the environment but the quantity required will be nearly 10 times more than that of silver and copper compounds. Enhancement of antibacterial activity of zinc compounds is being attempted by different groups, either by reducing the particle size or by incorporating heteroatoms in the matrix. Picconi *et al.*[1] demonstrated the antimicrobial potential of triarylbenzimidazoles against *Enterococci* and *Staphylococci* species. Sauad and his research team[2] evaluated the antibacterial property of calcium phosphate by measuring the inhibition zone of *S. aureus*. The antibacterial efficacy of calcium phosphate functionalized with aniline was determined by assessing its ability to prevent the growth of *E. coli* by Lorena *et al.*[3] The zinc phosphate nanoparticles were reported as a promising alternative for antibiotics owing to their antibacterial property in the literature.[4] Wu *et al.*[5] reported the antibacterial efficiency of hydroxyapatite and calcium phosphate against various bacteria species. The nanocomposite of bioactive glass and biphasic calcium phosphate was prepared to assess its antibacterial potential against *Salmonella typhi* and *E. coli*.[6] The minimum inhibitory concentration of Ag/SiO_2-based calcium phosphate against *S. aureus* was analyzed by performing the kinetics of colony-forming capacity assay and microbial growth analysis.[7] Yifan and his co-workers[8] studied the antimicrobial potential of Cu/phosphate-based glass nanoenzymes against gram-negative and gram-positive organisms and also demonstrated the antibacterial mechanism. The antimicrobial potential of Zn/zirconium phosphate glycinediphonate was evaluated against some pathogens causing orthopedic implant infections by Davide *et al.*[9] Zamperini and his research team[10] prepared the hydroxyapatite nanoparticles decorated with Ag to examine their antifungal property against *Candida albicans*. The various metal and metal oxides such as Y_2O_3,[11] Ag,[12] Fe_3O_4,[13] ZnO,[14] TiO_2,[15] and CuO[16] were investigated to assess their antimicrobial activities to inhibit the growth of a variety of harmful bacterial and pathogenic species. Diaz and his research group[17] studied the antibacterial property of Ag/hydroxyapatite against *E. coli, S. aureus,* and *Pneumococcus*. The biocomposite of Ag/cellulose was prepared and

http://doi.org/10.31788/RJC.2022.1526902

studied its bactericidal activity on drug-resistant bacterial strains.[18] Bankura *et al.*[19] inspected the antifungal property of Ag nanoparticles against *Candia albicans* fungi. The cationic Zn-porphyrin was investigated to assess its antifungal potential against *Saccharomyces cerevisiae* by Jayakumar *et al.*[20] The bimetallic Ag-Cu nanoparticles exhibited significantly higher antimicrobial activity as compared with Ag nanoparticles.[21] The medical devices implanted with Ag nanoparticles reduced the infection considerably due to the incorporation of an antibacterial agent.[22] The antimicrobial activity of the prepared silver nanoparticles using the leaf extracts of *Murraya koenigii* and *Feroniella lucida* was assessed against the pathogenic strains.[23,24] The antimicrobial activity of Cu nanoparticles[25] and tin(IV) complexes[26] was evaluated against *E. coli.* The study on the antibacterial and antifungal activities of zinc phosphate incorporated with Ag (AgZnP) is scarce in the open literature. Therefore, this study intends to analyze the bacterial growth-inhibiting potential of AgZnP against *E. coli and S. aureus* as well as its antifungal activity against *S. cerevisiae* and *A. brasiliensis.* The prepared antimicrobial agent of AgZnP exhibited a 5-fold increase in antimicrobial activity as compared with blank zinc phosphate.

EXPERIMENTAL

Preparation of Zinc Phosphate and Silver Activated Zinc Phosphate

The zinc phosphate was prepared by precipitation method by dissolving 66.8 g of zinc acetate (Aldrich Chemicals) in 200 mL of distilled water. Then, 0.5 g of cetyltrimethylammonium bromide (C-TAB, Aldrich Chemicals) was added to the above solution under stirring. In another beaker, 23g of orthophosphoric acid (Qualigens, 85%) was dispersed in 200 mL of distilled water. The phosphoric acid solution was slowly added to the zinc acetate solution under vigorous stirring to form fine precipitates of zinc phosphate. Afterward, it was kept in stirring condition for 60 min and further allowed to stand for 12 hrs. Then the precipitates were isolated upon centrifugation and washed with distilled water to remove unreacted acetate or soluble phosphate. The precipitate was dried at 150 °C for 4 h in an oven and it was calcined at different temperatures and labeled as ZnP. The preparation of silver activated zinc phosphate involves dissolving zinc acetate (66.8 g) and silver nitrate (0.66g, Aldrich chemicals) in a beaker and the rest of the procedure is the same as above. The samples were labeled as AgZnP.

Characterization

The X-ray diffraction patterns were recorded on a Bruker K 8600 instrument. The interaction of Ag with ZnP was concluded by recording the FTIR spectrum on Shimadzu 8400S, Japan for the prepared samples. The morphology of the AgZnP was examined by capturing SEM images using JSM6300, JEOL, USA.

Antibacterial Procedure

The minimum required concentration of AgZnP to inhibit the growth of *Staphylococcus aureus* (NCIM 2127) and *Escherichia coli* (NCIM 2931) was determined by the MIC dilution method. The bacterial counts were kept around 7.5×10^7 to carry out this analysis. The bacterial suspension in nutrient broth (without AgZnP) and the suspension of AgZnP in sterilized distilled water were employed as positive and negative controls respectively. Serially diluted quantities (between 1 mg and 50 mg) of the antibacterial samples were added into the tube containing bacterial suspension in nutrient broth and plugged with sterilized cotton. The tubes were incubated at 37°C for 24 h and observed for bacterial growth (appearance of turbidity). The minimum sample quantity in the tube which does not show bacterial growth (clear media) was reported at MIC for the sample. The antibacterial efficacy of the samples was evaluated by the ASTM-E-2149 method, where the bacterial suspension was added into a sterilized conical flask containing 50 mL of sterilized distilled water. Further, it was added to the prepared powder samples. The contents are plugged with sterilized non-absorbing cotton and shaken with a wrist shaker. Initially, in order to find the optimized contact time, 1 ml of the mixture was withdrawn at various time intervals and that was spread over a nutrient agar Petri plate using an 'L' rod. The contents are covered with another Petri plate and incubated for 24-48h. A blank analysis was made by adopting the above procedure without adding the sample. The percentage reduction of colony-forming units per mL (CFU/mL) was calculated for the sample by comparing it with the blank. This analysis was done thrice to check the variation in the results. The antifungal analysis was performed against *Saccharomyces*

cerevisiae (NCIM-3287, 9.55×10^5) and *Aspergillus brasiliensis* (NCIM-1196, 1.13×10^5) by adopting the above procedure and incubated for 5 days.

RESULTS AND DISCUSSION

XRD Analysis

The XRD patterns of the zinc phosphate and silver activated zinc phosphate calcined at 150°C, 250°C, and 350°C are given in Fig.-1a to f. The diffraction pattern of ZnP calcined at 150°C was in good agreement with JCPDS card No.33-1474 which confirmed the presence of zinc phosphate. On calcinations to 250°C, the hydrated water molecules leave to form α-$Zn_3(PO_4)_2$ (JCPDS card No.29-1390). The crystallinity of the zinc phosphate phase increased on further increasing calcinations temperature.[27]A similar type of XRD pattern was obtained for the silver activated zinc phosphate samples and no additional peaks representing the formation of silver oxide or silver phosphate were observed. This suggests that the silver would have been incorporated into the matrix of zinc phosphate. To confirm further, the unit cell parameters were calculated for the samples. The zinc phosphate hydrate present in the ZnP-150 and AgZnP-150 has orthorhombic symmetry. Considering the reflections at 2θ = 9.82 (020), 30.52 (051), and 31.58 (311), the d-spacing was calculated and substituting the values in the miller indices equation for orthorhombic crystal structure. The unit cell parameters were calculated and presented in Table-1. Similarly, the unit cell parameters for zinc phosphate in ZnP-350 and AgZnP-350 were calculated by considering monoclinic crystal structure and substituting d-spacing of the 2θ peaks = 19.5 (011), 22.51 (002) and 34.06 (220) in miller indices equation. The values are presented in Table-1. The unit cell volume for the zinc phosphate hydrate in ZnP-150 and AgZnP-150 was nearly the same with a marginal increase in the latter, while in the sample calcined at 350°C, there was a considerable increase in the unit cell volume due to a larger radius of silver ions (Ag^+ = 115 pm) in comparison with Zn^{2+} (74 pm).

Table-1: Unit Cell Parameters of ZnP and AgZnPCalcined at Different Temperatures

S.No.	ID	Unit cell parameters			
		a (Å)	b (Å)	c (Å)	V $(Å)^3$
1.	ZnP-150	10.4689	17.9996	5.0262	947.113
2.	Ag-ZnP-150	10.4935	17.9449	5.0324	947.615
3.	ZnP-350	15.7003	5.5814	8.1500	689.876
4.	Ag-ZnP-350	15.5701	5.6149	8.2147	693.729

FTIR Analysis

The FTIR spectra of the calcined zinc phosphate and silver-zinc phosphate at 150 °C and 350 °C are given in Fig.-1g to j. The peaks at 3400 and 1600 cm^{-1} for the calcined samples at 150 °C are due to the hydrated water molecules as inferred from the XRD analysis (Table-2). On increasing the calcination temperature, these vibrations disappear since anhydrous zinc phosphate is formed in ZnP-350 and Ag-ZnP-350 samples. The stretching of symmetric and anti-symmetric modes of PO_4^{3-} groups appears at around 1100 cm^{-1} and 1000 cm^{-1} respectively.[28,29] The $P\text{-}O^-$ bending vibration was reported to absorb at 960 cm^{-1}.[30]A decrease in the vibration frequency was observed for hydrated zinc phosphate as compared to anhydrous zinc phosphate. This may be due to a more stable orthorhombic crystal structure as compared with the former. Meantime, it is more stable as compared to the monoclinic structure of the latter.[31] On comparing the absorption between ZnP and AgZnP, the silver-activated sample showed a marginal decrease in value due to the incorporation of monovalent silver ions in the phosphate matrix.

Morphological Analysis by SEM

The scanning electron micrographs of ZnP-150 are given in Fig.-2a. The sample was found to have flower-like morphology (6-8 microns). On the other hand, the sample calcined at 350°C (ZnP-350) showed coalescence of the platelets, making it less porous (Fig.-2b). The AgZnP-150 exhibited a larger flower structure (10 – 12 microns) with distinct tiny platelets of around 150 nm (Fig.-2c(inset)). When this sample was calcined at 350°C, the flower size reduced to around 7–8 microns with coalescence of tiny platelets (Fig.-2d(in-set)). The morphology of both the samples, ZnP and AgZnP calcined at lower temperatures showed a distinct structure than that at higher temperatures.

Antibacterial Studies

The antibacterial analysis was carried out to find Minimum Inhibition Concentration (MIC) for ZnP and AgZnP samples calcined at 150 °C and 350 °C using the macrodilution method and the results are presented in Fig.-3(inset). It was concluded that the calcined samples at 350 °C exhibited enhanced antibacterial analysis as compared with that calcined at lower temperatures. The incorporation of silver in the matrix of zinc phosphate enhanced the antibacterial activity to a magnitude of 4 times. The bacterial reduction property of the samples was estimated according to the ASTM-E-2149 standard. The experiments were carried out at different contact times and the results are depicted in Fig.-3. The silver activated analogue exhibited very high activity within 10 minutes of contact time as compared to ZnP samples. However, after a contact time of around 50 minutes, all samples exhibited the same activity and the results are presented in Table 3 [*S. aureus* (Fig.-4a and b) and *E. coli* (Fig.-4c and d)].

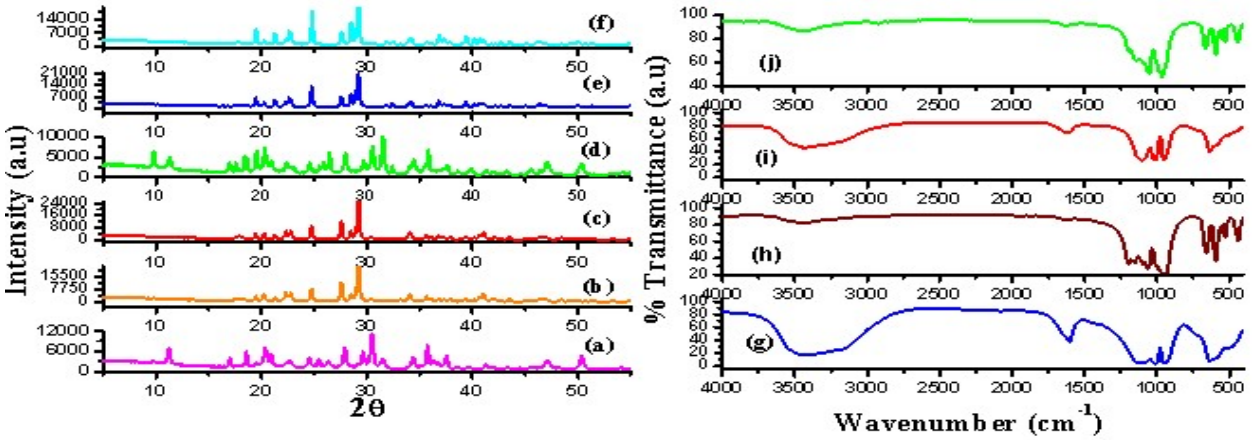

Fig.-1:XRD Patterns of ZnPCalcined at (a) 150°C (b) 250°C (c) 350°C and AgZnP Calcined at (d) 150°C (e) 250°C (f) 350°C; FTIR Spectra of ZnPCalcined at (g) 150°C (h) 350°C, and AgZnP Calcined at (i) 150°C (j) 350°C

Table-2: FTIR Vibrational Absorption of ZnP and AgZnP Calcined at Different Temperatures

S.No	ID→ Vibrations	ZnP-150 (cm^{-1})	AgZnP-150 (cm^{-1})	ZnP-350 (cm^{-1})	Ag-ZnP350 (cm^{-1})
1.	Vibrations due to hydrated water	3376 1593	3374 1590	--	--
2.	Symmetric stretching of PO_4^{3-}	1063	1093	1146	1106
3.	Antisymmetric stretching of PO_4^{3-}	958	953	1054	1045
4.	P-O bending	925	940	960	952

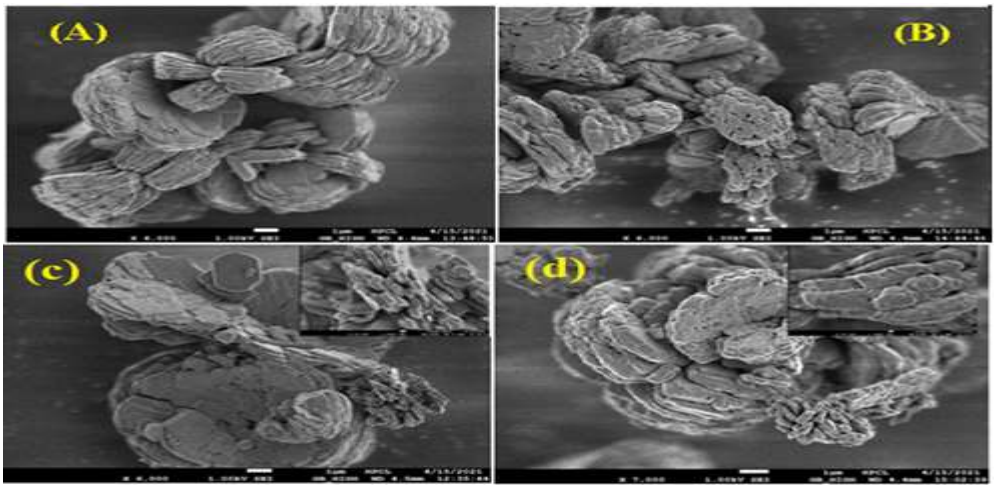

Fig.-2: SEM Micrographs of ZnP Calcined at (a) 150°C and (b) 350°C, AgZnP calcined at (c) 150°C and (d) 350°C

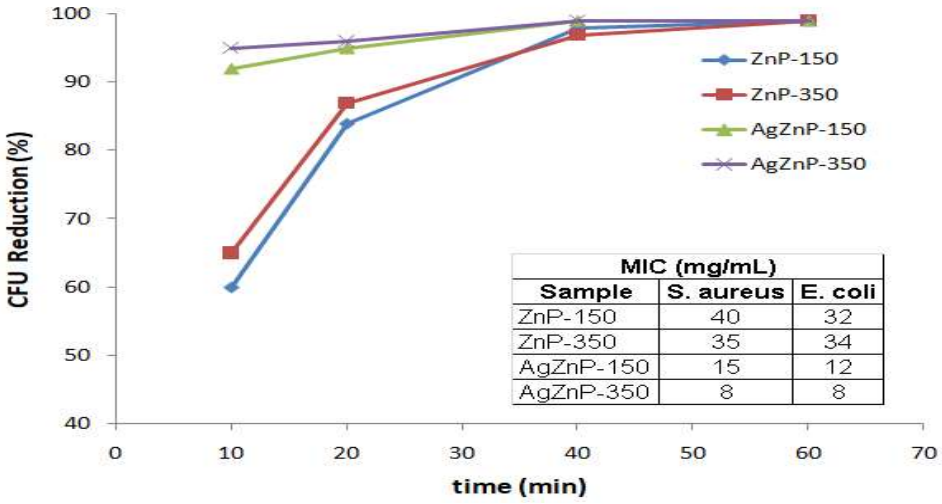

Fig.-3: Antibacterial Activity over ZnP and AgZnP samples: Effect of Contact Time

Antifungal Studies

The antifungal analysis was carried out against *S. cerevisiae* (Fig.-4e and f) and *A. brasiliensis* (Fig.-4g and h) and the results are presented in Table-3. The ZnP calcined at 350 °C exhibited better activity than that calcined at 150 °C. The silver activated zinc phosphate showed enhanced activity compared to the zinc analogue. This proved its efficiency against fungal growth also.

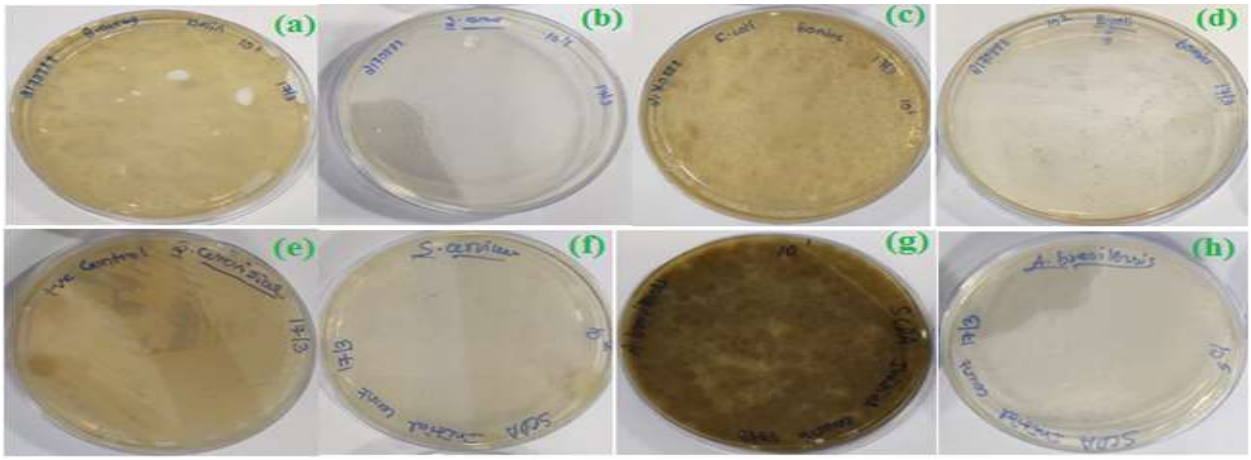

Fig.-4: Antibacterial Analysis Against *S. aureus* (a) Blank and (b) AgZnP-350; against *E. coli* (c) Blank (d) AgZnP-350; Antifungal Analysis against *S. cerevisiae* (e) Blank and (f) AgZnP-350; against *A. brasiliensis*(g) Blank (h) AgZnP-350

Table-3: Antimicrobial Analysis of ZnP and AgZnP Samples Calcined at Different Temperatures.

SN	Sample ID	Antibacterial Analysis		Antifungal Analysis	
		S. aureus	*E. Coli*	*S. cerevisiae*	*A. brasiliensis*
1.	ZnP-150	97.9	97.8	96.2	97.1
2.	ZnP-350	98.5	98.2	97.7	98.9
3.	AgZnP-150	99.9	99.9	99.8	99.9
4.	AgZnP-350	99.9	99.9	99.9	99.9

* The variation in CFU reduction % results is ± 1.0%.

CONCLUSION

Zinc phosphate was prepared using the chemical precipitation technique. To enhance the antibacterial activity, silver was incorporated into the matrix. The XRD analysis proved the presence of zinc phosphate hydrate in the ZnP and AgZnP samples calcined at 150 °C, however, it was converted to zinc phosphate

at 250°C. No additional phases of silver oxide or silver phosphate were observed, suggesting the incorporation of silver in the zinc phosphate matrix. The unit cell parameters were calculated for both the samples and an increase in the unit cell volume was observed for silver activated analogue. The FTIR vibrational analysis showed a decrease in the value for AgZnP as compared to ZnP proving the interaction of silver with the phosphate matrix. The SEM analysis showed flower-like morphology for the sample calcined at 150°C which coalesced on increasing the calcination temperature. The MIC values for silver activated analogue was found to be 4 times lesser than the zinc phosphate and showed a maximum activity with much better contact time. The sample was also found to exhibit appreciable antifungal activity.

REFERENCES

1. P. Picconi, C. Hind, S. Jamshidi, K. Nahar, M. Clifford, M.E. Wand, J. Mark Sutton, and Khondaker Miraz Rahma, *Journal of Medicinal Chemistry*, **60**, 6045(2017), https://doi.org/10.1021/acs.jmedchem.7b00108
2. G. Souad, and C. Baghdadi, *Material Research Express*, **7**, 015040(2020), https://doi.org/10.1088/2053-1591/ab6260
3. B. Lorena Polo, de Greñu, S. Pagani, P. Torricelli, J. Luis Vivancos, M. Ruiz-Rico, J. M. Barat, E. Aznar, R. Martínez-Máñez, and M. Fini, *Acta Biomaterialia*, **81**, 293(2018), https://doi.org/10.1016/j.actbio.2018.09.033
4. P. Horky, S. Skalickova, L. Urbankova, D. Baholet, S. Kociova, Z. Bytesnikova, E. Kabourkova, Z. Lackova, N. Cerne, M. Gagic, V. Milosavljevic, V. Smolikova, E. Vaclavkova, P. Nevrkla, P. Knot, O. Krystofova, D. Hynek, P. Kopel, J. Skladanka, V. Adam, and K. Smerkova, *Journal of Animal Science and Biotechnology*, **10**, 17(2019), https://doi.org/10.1186/s40104-019-0319-8
5. V. M. Wu, S.Tang, and V. Uskoković, *ACS Applied Materials & Interfaces,* **10**, 34013(2018), https://doi.org/10.1021/acsami.8b12784
6. N. Zahra, M. N. Mehdi, H. N. Masoumeh, S. Hamid, K. Mohammad Mehdi, *Applied Physics: A*, **122**, 1063(2016), https://doi.org/10.1007/s00339-016-0587-5
7. J. Kung, W. Wang, C. Lee, H. Hsieh, and C. Shih, *Nanomaterials*, **10**,1264(2020), https://doi.org/10.3390/nano10071264
8. L. Yifan, N. Nie, H. Tang, C. Zhang, K. Chen, W. Wang, and J. Liu, *ACS Applied Materials & Interfaces*, **13**, 11631(2021), https://doi.org/10.1021/acsami.0c22746
9. C. Davide, S. Ravaioli, R. Vivani, A. Donnadio, E. Vischini, A. Russo, L. Visai, C. Renata Arciola, L. Montanaro, and M. Nocchetti, *Materials*, **12**, 3184(2019), https://doi.org/10.3390/ma12193184
10. C. A. Zamperini, R. S. André, V. M. Longo, E. G. Mima, C. E. Vergani, A. L. Machado, J. A. Varela, and E. Longo, *Journal of Nanomaterials*, **Volume 2013**, 174398(2013), https://doi.org/10.1155/2013/174398
11. S. H. Cha, J. Hong, M. McGuffie, B. Yeom, J.S. VanEpps, and N.A. Kotov, *ACS Nano*, **9**, 9097(2015), https://doi.org/10.1021/acsnano.5b03247
12. L. Actis, A. Srinivasan, J. L. Lopez-Ribot, A.K. Ramasubramanian, and J. L. Ong, *Journal of Materials Science: Materials in Medicine*, **26**, 215(2015), https://doi.org/10.1007/s10856-015-5538-8
13. M. Arakha, P. Sweta, S. Devyani, T. K. Panigrahi, C. Bairagi, Mallick, K. Pramanik, B. Mallick, and S. Jha, *Scientific Reports,* **5**,14813(2015), https://doi.org/10.1038/srep14813
14. S. Mehmood, M. A. Rehman, H. Ismail, B. Mirza, A. S. Bhatti, *International Journal of Nanomedicine*, **10**, 4521(2015), https://doi.org/10.2147/IJN.S83356
15. S. Rezaei-Zarchi, A. Javed, G. Javeed, S. Soufian, F. Barzegari, M. Bayanduri, *Iranian Journal of Pathology*, **5**, 83(2010)
16. V.V. ThekkaePadil, and M. Cernik, *International Journal of Nanomedicine*, **8**, 889(2013), https://doi.org/10.2147/IJN.S40599
17. M. Díaz, F. Barba, M. Miranda, F. Guitián, R. Torrecillas, and J. S. Moya, *Journal of Nanomaterials*, **498505**, 1(2009), https://doi.org/10.1155/2009/498505
18. J. A. Garza-Cervantes, G. Mendiola-Garza, E. M. De Melo, T. I. J. Dugmore, A. S. Matharu, and J. R. Morones-Ramirez, *Scientific Reports,* **10**, 7281(2020), https://doi.org/10.1038/s41598-020-64127-9

19. K. P. Bankura, D. Maity, M. M. R. Mollick, D. Mondal, B. Bhowmick, M. K. Bain, A. Chakraborty, J. Sarkar, K. Acharya, and D. Chattopadhyay, *Carbohydrate Polymers,* **89**, 1159(2012), https://doi.org/10.1016/j.carbpol.2012.03.089
20. S. Jayakumar, H. Li, L. Tao, C. Li, L. Liu, J. Chen, and Q. Yang, *ACS Sustainable Chemical Engineering*, **6**, 9237(2018), https://doi.org/10.1021/acssuschemeng.8b01548
21. T. Merve, S. Nilufer, G.Y. Isik, and S. Sefik, *Journal of Materials Chemistry*, **21**, 13150(2011), https://doi.org/10.1039/C1JM11718A
22. F. Furno, K.S. Morley, B. Wong, B.L. Sharp, and S.M. Howdle, *Journal of Antimicrobial Chemotherapy*, **54**, 1019(2004), https://doi.org/10.1093/jac/dkh478
23. P. Sankarganesh, A. Ganesh Kumar, V. Parthasarathy, Baby Joseph, G. Priyadharsini and R. Anbarasan, *Journal of Inorganic and Organometallic Polymers and Materials,* **31**, 2971(2021), https://doi.org/10.1007/s10904-021-01894-6
24. A. Ganesh Kumar, P. Sankarganesh, V. Parthasarathy, J. Bhuvaneshwari and R. Anbarasan, *Journal of Sol-Gel Science and Technology,* **101**, 411(2022), https://doi.org/10.1007/s10971-022-05728-w
25. N. Karikalan, *Rasayan Journal of Chemistry,* **11**, 1451(2018), https://doi.org/10.31788/RJC.2018.1143068
26. P. Yadav, R. Meena, and B.S. Joshi, *Rasayan Journal of Chemistry,* **14**, 1240(2021), http://dx.doi.org/10.31788/RJC.2021.1426168
27. Z.R. Liu, R.X. Zhong, H. Zhao, and X.Y. Zhang, **423–426**, 415(2013), https://doi.org/10.4028/www.scientific.net/AMM.423-426.415
28. S.P. Yan, W. He, and C.Y. Sun, *Dyes and Pigments*, **80**, 254(2009), https://doi.org/10.1016/j.dyepig.2008.06.010
29. M. Zhang, J.K. Liu, R. Miao, G.M. Li, and Y.J. Du, *Nano-scale Research Letters*, **5**, 675(2010), https://doi.org/10.1007/s11671-010-9530-4
30. J. Seung-Ho, O. Eugene, S. Daeseob, P. Da-Hye, C. Seungho, L. Bo Ram, J. Yeon, L. Kun-Hong, and J. Soo-Hwan, *Bulletin of the Korean Chemical Society*, **30**, 2280(2009), https://doi.org/10.5012/BKCS.2009.30.10.2280
31. Zhi-Gang Mei, Shun-Li Shang, Yi Wang, and Zi-Kui Liu, *Journal of Physics: Condensed Matter,***22**, 295404(2010), https://doi.org/10.1088/0953-8984/22/29/295404

[RJC-6902/2021]